Measurement of EUV spectra from high Z elements in the Large Helical Device

C. Suzuki*, T. Kato*, H. A. Sakaue*, D. Kato*, I. Murakami*, K. Sato*, N. Tamura*, S. Sudo*, N. Yamamoto†, H. Tanuma**, H. Ohashi**, R. D'Arcy‡, C. S. Harte‡ and G. O'Sullivan‡

*National Institute for Fusion Science, 322-6 Oroshi-cho, Toki 509-5292, Japan
†Institute of Laser Engineering, Osaka University, 2-6 Yamadaoka, Suita 565-0871, Japan
**Tokyo Metropolitan University, 1-1 Minami-Osawa, Hachioji 192-0397, Japan
‡University College Dublin, Belfield, Dublin 4, Ireland

Abstract. Extreme ultra-violet (EUV) emission spectra from highly charged tin, xenon and tungsten ions have been measured in optically thin high-temperature plasmas produced in the Large Helical Device (LHD) at the National Institute for Fusion Science by using a grazing incidence spectrometer and a tracer-encapsulated solid pellet (TESPEL) injector. Quasi-continuous spectral features arising from unresolved transition array (UTA) of open 4d subshell ions were commonly observed for tin, xenon and tungsten around 13.5, 11, and 5 nm, respectively, when edge plasma was cooled enough. The spectral appearance obviously depends on edge electron temperature and atomic number. In the case of intermediate edge temperature, sharp discrete lines from highly charged open 4s or 4p subshell ions are clearly observed for tin and xenon in longer wavelength side of the UTAs but not for tungsten. Assignments of the strong discrete lines have been performed with the help of comparisons with the other experimental data and the theoretical calculations by Cowan code. Contribution of open 4f subshell ions should also be considered to interpret the whole spectra from tungsten ions.

Keywords: LHD, EUV Spectra, High Z elements, Highly charged ions, Tin, Xenon, Tungsten
PACS: 31.15.ag, 32.30.Rj, 32.70.Fw, 52.25.Os, 52.55.Hc

INTRODUCTION

The Large Helical Device (LHD) is a large-scale facility for magnetically confined torus plasma experiment at the National Institute for Fusion Science, in which high temperature ($>$1 keV) and optically thin ($n_e \simeq 10^{18}$–10^{20} m^{-3}) hydrogen plasmas are routinely produced by a sufficient heating power [1]. LHD plasmas can be considered as a characteristic light source including substantial extreme ultra-violet (EUV) emissions from highly charged ions of any high-Z impurity injected intentionally by pellet or gas puff. It is an advantage of LHD that the effects of line broadening and self absorption tend to be relatively weak in contrast to laser produced high density plasmas. In addition, detailed information on electron temperature/density profiles can be obtained from Thomson scattering diagnostic [2]. These properties make the LHD an advantageous source of experimental database of EUV spectra from various elements for benchmarking with theoretical calculations of spectral lines.

In this context, atomic/molecular physics is regarded as an important subject in LHD project in that it has been selected as one of the physics oriented theme groups in LHD experimental campaign. It includes applications not only for fusion science, but also

for other research fields such as plasma application and astrophysics. In this study we will focus on the measurements of EUV spectra from highly charged tin, xenon and tungsten ions which have recently drawn considerable attention. Tin and xenon have been investigated as candidate elements in the development of EUV light source for the next generation semiconductor lithography [3, 4], and tungsten has been determined as a plasma facing component in the forthcoming International Thermonuclear Experimental Reactor (ITER) project [5]. We have measured EUV spectra from these elements in LHD so far [6, 7, 8, 9].

Note that contribution of open N shell (n=4) ions are commonly important in these elements. In general, these ions with open 4d subshell electrons tend to constitute strong quasi-continuous emission overlaid by many lines due to $4p^6 4d^m$–$4p^5 4d^{m+1}$ + $4p^6 4d^{m-1} 4f$ transitions in EUV wavelength region, which is often referred to as unresolved transition array (UTA) [10]. On the other hand, open 4s or 4p subshell ions are considered to constitute different spectrum consisting of strong discrete lines because the number of energy levels are relatively smaller than that of open 4d subshell ions. Therefore the UTA features are observed especially under the conditions that the dominant ion charge states are relatively low, while discrete lines are expected when the dominant charge states are higher.

The experimental measurements and analyses of the quasi-continuous and discrete spectral features in LHD are reviewed in this study. The assignments of the spectral lines and features have been carried out by comparisons with previous articles, charge exchange collisions experiment [11], and theoretical calculations with the Hartree-Fock Configuration Interaction (HFCI) code of Cowan [12].

EXPERIMENTAL

The LHD plasma is confined by a strong magnetic field generated by several superconducting helical and poloidal coils. The major and minor radii of the torus plasma are typically 3.75 m and 0.6 m, respectively, which results in a huge plasma volume ($\simeq$30 m^3) [1]. The magnetic field strength used in this study is typically 2.75 T at the plasma center. A small amount ($\simeq$0.1 % of bulk ion) of solid tin or tungsten was introduced into the hydrogen plasma by injecting a tracer encapsulated solid pellet (TESPEL) [13], while xenon was introduced by a gas puffing. Spatial profiles of electron density and temperature were measured by a laser Thomson scattering diagnostic system [2]. The EUV spectra were recorded by a Schwob-Fraenkel type grazing incidence spectrometer SOXMOS [14] whose groove density and focal length are 600 mm^{-1} and 1 m, respectively. The overall spectral resolution was about 0.01 nm. Bright emissivity of the LHD plasma enables us to utilize short exposure time such as 0.2 s, and temporal evolution of the spectrum can be traced during long pulse duration of several seconds. The wavelength of the spectrometer was calibrated by observing the known lines of iron, argon and neon ions from plasmas with injection of these elements. Consequently, we could determine the absolute wavelength with an accuracy of $\pm$0.01 nm.

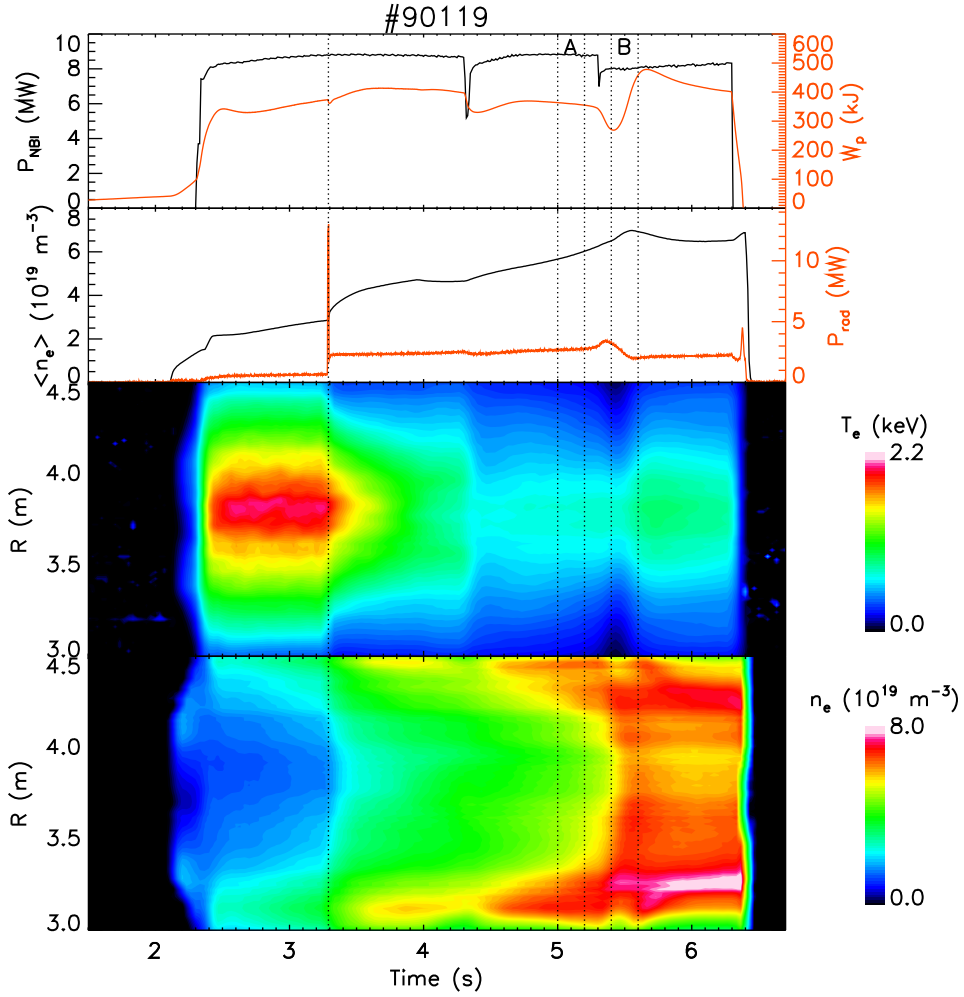

FIGURE 1. Time evolutions of neutral beam injection heating power (P_{NBI}), stored energy (W_p), line averaged electron density ($\langle n_e \rangle$), and total radiated power (P_{rad}), and contour plots of electron temperature (T_e) and density (n_e) profiles from edge (R = 3.1 or 4.4 m) to core (R = 3.75 m) in a discharge with a tin pellet injection at 3.3 s. There was an edge cooling event at around 5.4–5.5 s as indicated by dips of the stored energy and the contour of electron temperature. EUV spectra measured during the periods A (5.0–5.2 s) and B (5.4–5.6 s) are shown in Fig. 2.

OBSERVED SPECTRA

EUV spectra have been observed mainly in the wavelength ranges around 13.5 nm, 11 nm and 5 nm for tin, xenon and tungsten, respectively, where emissions from open N shell ions are expected. The measured spectral appearance sometimes drastically changes according to change in electron temperature near the edge region. An example of such a situation in a discharge with a tin pellet injection is described in Figs. 1 and 2.

Figure 1 shows time evolutions of neutral beam injection heating power (P_{NBI}), stored energy (W_p), line averaged electron density ($\langle n_e \rangle$) and total radiated power (P_{rad}) in the top 2 panels. Time evolutions of electron temperature and density profiles from edge (R

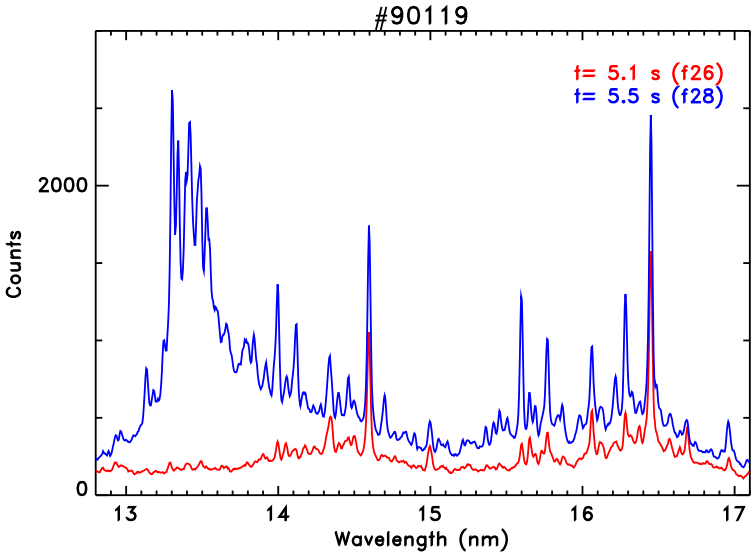

FIGURE 2. The two distinct EUV spectra from tin ions in 13–17 nm measured during the periods A (5.0–5.2 s, red) and B (5.4–5.6 s, blue) in the discharge shown in Fig. 1.

= 3.1 or 4.4 m) to core (R = 3.75 m) region are drawn as contour plots in the bottom 2 panels. The tin pellet was injected at 3.3 s.

It is notable that an event was triggered by a sudden decrease in heating power at around 5.4 s where dips of the stored energy and edge electron temperature were observed. Because the electron density did not decrease during this event, this indicates that dense cold region would be formed near the edge around 0.1 m inside from the plasma boundary (R $\simeq$ 3.1 m and 4.4 m). This results in a drastic change in the spectral appearance between the two time periods A (5.0–5.2 s) and B (5.4–5.6 s) as shown in Fig. 2. Only sharp discrete lines were observed in the range of 14–17 nm before the event. When the plasma edge is cooled as low as 200 eV, a broad spectral feature arising from UTA of open 4d subshell ions appears around 13.5 nm. As described in the next section, most of the sharp discrete lines in longer wavelength region are from higher charge states with open 4s or 4p subshell ions [8].

A similar example for the tungsten case is shown in Figs. 3 and 4, where the pellet was injected at 2.3 s and edge plasma was cooled at around 2.8 s. EUV spectra around 5 nm during the periods A (2.4–2.6 s), B (2.8–3.0 s) and C (5.0–5.2 s) are plotted in Fig. 4 by red, blue and green lines, respectively. In contrast to tin, main broad spectral feature near 5.0 nm and smaller broad peak around 6.0 nm are commonly dominant in all the periods, and the discrete feature was not clear even under the higher temperature condition. It is noted that the strong line group between 4.9 and 5.1 nm is especially pronounced only when the temperature increased again at 5.0 s by an additional heating power. However, these lines are not due to open 4s or 4p subshell ions as shown later.

The intermediate situation is the case for xenon. The discrete lines arising from open 4s or 4p subshell xenon ions become more intense in the longer wavelength side in higher temperature case though a trace of the quasi-continuous feature still

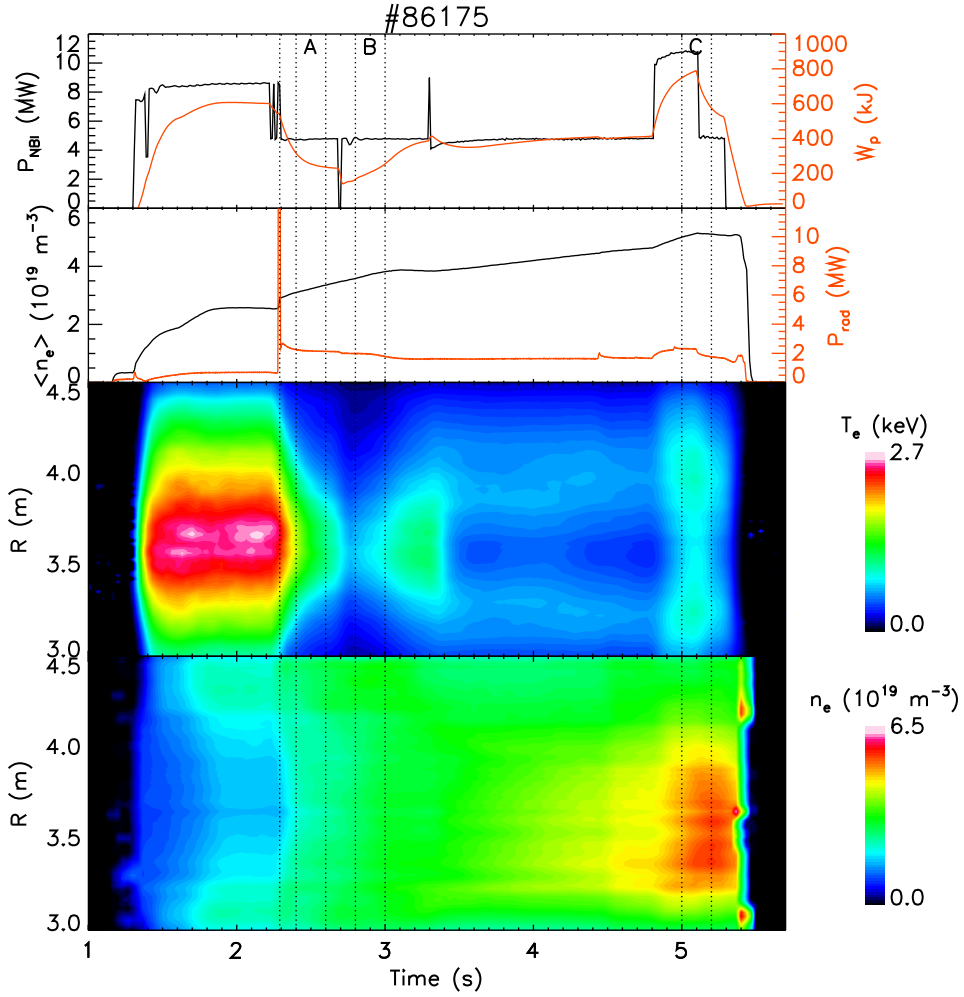

FIGURE 3. Time evolutions of the parameters in a discharge with a tungsten pellet injection at 2.3 s. Contour plots of the electron temperature/density from edge to core (R = 3.60 m) region are also illustrated. Plasma edge was cooled at around 2.8 s, and heated around 5.0 s by an additional input power. EUV spectra measured during the periods A (2.4–2.6 s), B (2.8–3.0 s) and C (5.0–5.2 s) are shown in Fig. 4.

remains around 10.8 nm. When the edge plasma was cooled, quasi-continuous feature is completely dominant against the discrete lines.

This dependence of the spectral feature on edge electron temperature and atomic number can be qualitatively understood by the difference in ionization potentials of the charge states relevant to each spectral feature of the EUV emission as shown in Fig. 5 as a function of the number of electrons [15, 16]. In general, open 4s or 4p subshell ions, in which the number of electrons is 29–36, contribute to the discrete line spectral feature because of smaller number of electrons and energy levels in subshells relevant to EUV emission, while open 4d subshell ions, in which the number of electrons is 37–46, are related to the UTA feature because of very large number of energy levels in the subshell. The ionization potentials of open 4s or 4p subshell ions are approximately 300–900 eV

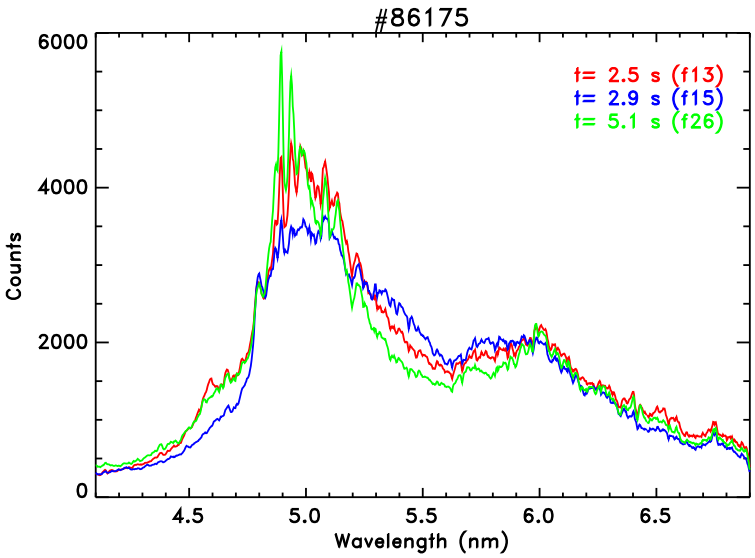

FIGURE 4. The measured EUV spectra from tungsten ions around 5 nm during three different periods A (2.4–2.6 s, red), B (2.8–3.0 s, blue) and C (5.0–5.2 s, green) in the discharge shown in Fig. 3.

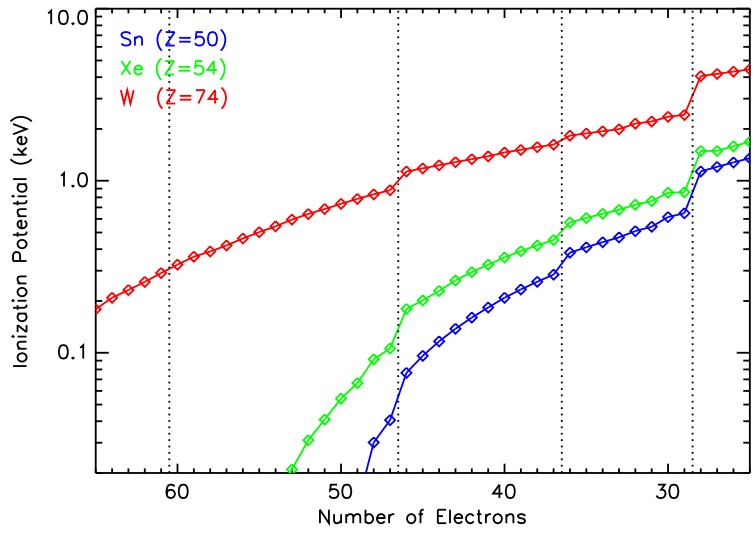

FIGURE 5. Ionization potentials of tin, xenon, and tungsten ions as a function of the number of electrons.

for tin and xenon, respectively, but 1800–2400 eV for tungsten. Therefore it is difficult to observe the discrete spectral lines of tungsten even in higher electron temperature cases in LHD. Certainly, discrete lines due to open 4s or 4p subshell tungsten ions were clearly observed under the condition of much higher electron temperature in other tokamak devices [5, 17].

TABLE 1. List of spectral lines from of Cu-, Zn- and Ga-like tin and xenon identified in LHD spectra.

		Sn		Xe	
	Transition	λ_{LHD} (nm)	Ref.	λ_{LHD} (nm)	Ref.
Cu-like	$4p\ ^2P_{1/2} - 4d\ ^2D_{3/2}$	14.596	[22]	11.902	[23]
	$4d\ ^2D_{3/2} - 4f\ ^2F_{5/2}$	15.646	[22]		
	$4d\ ^2D_{5/2} - 4f\ ^2F_{7/2}$	16.055	[22]		
	$4p\ ^2P_{3/2} - 4d\ ^2D_{5/2}$	16.441	[22]	13.839	[23]
	$4p\ ^2P_{3/2} - 4d\ ^2D_{3/2}$	16.946	[22]		
Zn-like	$4p\ ^3P_2 - 4d\ ^3D_3$	15.764	[24]	13.251	[25]
	$4p\ ^1P_1 - 4d\ ^1D_2$	16.274	[24]	13.623	[25]
Ga-like	$4s^24p\ ^2P_{1/2} - 4s^24d\ ^2D_{3/2}$	13.999	(this work)	11.368	[26]
	$4s^24p\ ^2P_{3/2} - 4s^24d\ ^2D_{5/2}$	15.593	(this work)	13.066	[26]

ANALYSES

The analyses of the UTA structure for tin and xenon are not discussed here because they have already been done in detail [6, 18, 19, 20]. In this study, assignments of the strong discrete lines from tin and xenon ions, and the complicated broad features of tungsten ions have been performed with the help of comparisons with the previous experimental results, the experimental spectra in charge exchange collisions [21] and the theoretical calculations by Cowan code.

Consequently, most of the strong discrete lines in longer wavelength side of the UTAs from tin and xenon have been assigned to the 4p-4d or 4d-4f transitions of higher charge states with open 4s or 4p subshell Cu- to Ge-like ions [8], which are partially summarized in table 1. It is noteworthy that the lines of Cu-like and Zn-like ions due to transitions between excited states are clearly observed in LHD, which are only very weakly observed in electron beam ion traps (EBITs) because of extremely low density. Though lines from 4p-4d transitions of Ga- and Ge-like tin ions are also superposed in Fig. 2, there is no previous data available for these ions. Hence the theoretical calculations were performed for 4p-4d transitions of Sn XX and Sn XIX ions using the Cowan code. Consequently, we have succeeded to assign most of the remaining strong spectral lines to these ions. Many lines of Ge-like ions are also found and listed in ref. [8]. It should be emphasized that the lines from Ga- and Ge-like tin were identified for the first time in this work. The identifications of Zn-like and Ga-like tin ions have also been validated by spectra obtained in the charge exchange collisions experiment [21], and also by analyses of temporal variations of line intensities in the discharge. Though the calculated wavelengths for Ga and Ge-like tin lines are systematically shifted by longer wavelength in comparison with the measured ones, it can be attributed to an overestimation in Slater Condon parameters and the lack of scaling of the spin-orbit integrals in the calculation.

In the case of tungsten, a few strong peaks are superposed on the broad UTA feature around 5.0 nm especially in higher temperature case as shown in Fig. 4. Three peaks between 4.9–5.0 nm can be attributed to the previously identified 4d-4f resonance lines

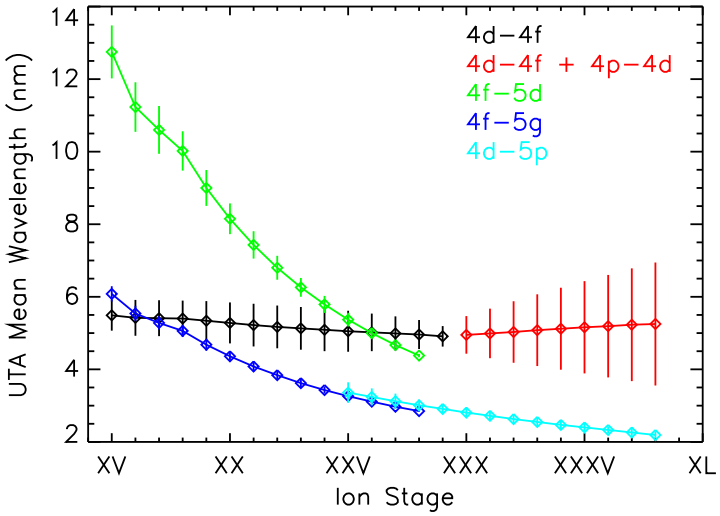

FIGURE 6. Mean position and array widths (expressed by vertical bars) of UTAs for 4d-4f, 4d-5p, 4f-5g and 4f-5d transitions in a range of open 4f and 4d subshell tungsten ions.

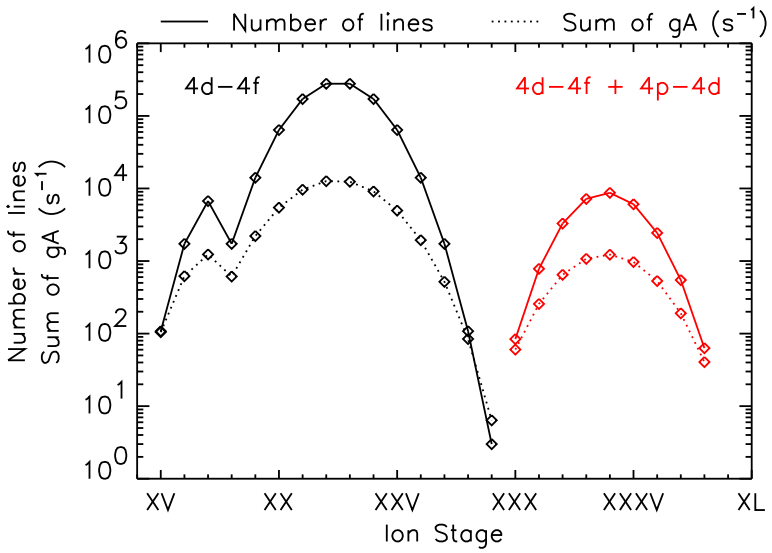

FIGURE 7. The calculated number of lines and sum of statistically weighted transition probability (*gA*) for 4d-4f (+ 4p-4d) transitions in a range of open 4f (black) and open 4d (red) subshell tungsten ions.

of Ag- to Rh-like tungsten ions [27, 28, 29, 30], and strong discrete lines of open 4s or 4p subshell ions are not clearly observed in Fig. 4. A smaller broad peak structure appearing around 6 nm region is quite noticeable, which are also observed in other experiments in fusion plasmas [5, 31, 32]. Furthermore, Berlin EBIT group also observed similar unknown broad structure around 6 nm at electron beam energies corresponding

to ionization energy of open 4f tungsten ions [33]. These facts suggest large contribution of lower charged open 4f subshell ions in the tungsten spectra observed in LHD. Although open 4f tungsten ions would be important in edge region of fusion plasmas, experimental/theoretical data for these ions are still insufficient [16]. Calculations and assignments of open 4f tungsten ions are challenging because of complexity of energy levels and spectral feature.

To further investigate the contribution of various transitions to the structure, we have carried out detailed calculations for open 4f tungsten ions by the Cowan code with a modification for numerous number of lines [9]. Consequently mean position and array widths of UTAs for 4d-4f, 4d-5p, 4f-5g and 4f-5d transitions are summarized graphically for all of the open 4f and 4d tungsten ions in Fig. 6. Calculated number of lines and sum of *gA* (statistically weighted transition probability) are plotted in Fig. 7 for 4d-4f (+ 4p-4d) transitions of open 4f and 4d tungsten ions, which indicates enormous line density resulting from the presence of the open 4f subshell.

As a result, large contribution of open 4f subshell ions to the broad structure around 5 nm is suggested as well as open 4d ions. The smaller broad peak observed around 6 nm which is absent from Fig. 4 cannot be explained only by the 4d-4f transitions. This structure can be associated with 4f-5d transitions in W XXIII–XXIV as well as some 4d-4f + 4p-4d transitions in W XXXV–XXXVIII. The absence of 4f-5d transitions at longer wavelengths is most likely associated with the presence of configurations containing one or two 5s electrons or low populations of stages lower than W^{21+} or both. Further investigation is necessary for the interpretation of the whole spectral feature of tungsten ions.

SUMMARY

We have observed EUV spectra from highly charged tin, xenon and tungsten ions in optically thin high-temperature LHD plasmas by using TESPEL injector and SOXMOS spectrometer. The measured spectral appearance largely depends on electron temperature near the plasma edge and atomic number of the element. Quasi-continuous UTA features from open 4d subshell ions were commonly observed for tin, xenon and tungsten in EUV region when edge plasmas are cooled as low as 200 eV. In higher temperature plasmas, discrete line spectral feature was clearly observed for tin and xenon, but not clearly observed for tungsten. Most of the strong spectral lines from tin and xenon ions have been assigned to Cu- to Ge-like ions with the help of previous experimental observations, charge exchange collision experiment and Cowan code calculation. Sn XX and XIX lines have been identified for the first time in this study. The observed tungsten spectra and comparisons with Cowan code calculation indicate large contribution of open 4f subshell ions which should be investigated further experimentally and theoretically because of its importance in fusion edge plasmas.

ACKNOWLEDGMENTS

The authors acknowledge the LHD experiment group for their assistance. This work was partly supported by the MEXT under the leading project for EUV lithography source development, and the Science Foundation Ireland under Grant No. 08/RFP/PHY1100.

REFERENCES

1. A. Komori et al., *Nucl. Fusion* **49**, 104015 (2009).
2. K. Narihara, I. Yamada, H. Hayashi, and K. Yamauchi, *Rev. Sci. Instrum.* **72**, 1122 (2001).
3. V. Bakshi, *EUV Sources for Lithography*, SPIE, Bellingham, 2006.
4. K. Nishihara et al., *Phys. Plasmas* **15**, 056708 (2008).
5. T. Pütterich, R. Neu, R. Dux, A. D. Whiteford, M. G. O'Mullane, and the ASDEX Upgrade Team, *Plasma Phys. Control. Fusion* **50**, 085016 (2008).
6. T. Kato et al., *J. Phys. B: At. Mol. Opt. Phys.* **41**, 035703 (2008).
7. C. Suzuki, T. Kato, K. Sato, N. Tamura, D. Kato, S. Sudo, N. Yamamoto, H. Tanuma, H. Ohashi, S. Suda, G. O'Sullivan, and A. Sasaki, *J. Phys.: Conf. Ser.* **163**, 012019 (2009).
8. C. Suzuki, T. Kato, H. A. Sakaue, D. Kato, K. Sato, N. Tamura, S. Sudo, N. Yamamoto, H. Tanuma, H. Ohashi, R. D'Arcy, and G. O'Sullivan, *J. Phys. B: At. Mol. Opt. Phys.* **43**, 074027 (2010).
9. C. S. Harte, C. Suzuki, T. Kato, H. A. Sakaue, D. Kato, K. Sato, N. Tamura, S. Sudo, R. D'Arcy, E. Sokell, J. White, and G. O'Sullivan, *J. Phys. B: At. Mol. Opt. Phys.* **43**, 205004 (2010).
10. G. O'Sullivan, and R. Faulkner, *Opt. Eng.* **33**, 3978 (1994).
11. H. Tanuma, H. Ohashi, E. Shibuya, N. Kobayashi, T. Okuno, S. Fujioka, H. Nishimura, and K. Nishihara, *Nucl. Instr. and Meth. in Phys. Res. B* **235**, 331 (2005).
12. R. D. Cowan, *The Theory of Atomic Structure and Spectra*, University of California Press, Berkeley, 1981.
13. S. Sudo et al., *Plasma Phys. Control. Fusion* **44**, 129 (2002).
14. J. L. Schwob, A. W. Wouters, S. Suckewer, and M. Finkenthal, *Rev. Sci. Instrum.* **58**, 1601 (1987).
15. E. B. Saloman, *J. Phys. Chem. Ref. Data* **33**, 765 (2004).
16. A. E. Kramida, and T. Shirai, *At. Data Nucl. Data Tables* **95**, 305 (2009).
17. T. Nakano, N. Asakura, H. Kubo, J. Yanagibayashi, and Y. Ueda, *Nucl. Fusion* **49**, 115024 (2009).
18. S. S. Churilov, Y. N. Joshi, J. Reader, and R. R. Kildiyarova, *Phys. Scr.* **70**, 126 (2004).
19. S. S. Churilov, and A. N. Ryabtsev, *Phys. Scr.* **73**, 614 (2006).
20. R. D'Arcy, H. Ohashi, S. Suda, H. Tanuma, S. Fujioka, H. Nishimura, K. Nishihara, C. Suzuki, T. Kato, F. Koike, J. White, and G. O'Sullivan, *Phys. Rev. A* **79**, 042509 (2009).
21. H. Ohashi, S. Suda, H. Tanuma, S. Fujioka, H. Nishimura, A. Sasaki, and K. Nishihara, *J. Phys. B: At. Mol. Opt. Phys* **43**, 065204 (2010).
22. J. Reader, N. Acquista, and D. Cooper, *J. Opt. Soc. Am.* **73**, 1765 (1983).
23. V. Kaufman, J. Sugar, and W. L. Rowan, *J. Opt. Soc. Am. B* **5**, 1273 (1988).
24. C. M. Brown, J. F. Seely, D. R. Kania, B. A. Hammel, C. A. Back, R. W. Lee, A. Bar-Shalom, and W. E. Behring, *At. Data Nucl. Data Tables* **58**, 203 (1994).
25. H. H. Hacker et al., *Appl. Phys. B* **73**, 59 (2001).
26. C. Biedermann, R. Radtke, G. Fußmann, J. L. Schwob, and P. Mandelbaum, *Nucl. Instr. and Meth. in Phys. Res. B* **235**, 126 (2005).
27. K. Asmussen, K. B. Fournier, J. M. Laming, R. Neu, J. F. Seely, R. Dux, W. Engelhardt, J. C. Fuchs, and ASDEX Upgrade Team, *Nucl. Fusion* **38**, 967 (1998).
28. J. Sugar, V. Kaufman, and W. Rowan, *J. Opt. Soc. Am. B* **10**, 799 (1993).
29. J. Sugar, V. Kaufman, and W. Rowan, *J. Opt. Soc. Am. B* **10**, 1321 (1993).
30. J. Sugar, V. Kaufman, and W. Rowan, *J. Opt. Soc. Am. B* **10**, 1977 (1993).
31. R. Isler, R. Neidigh, and R. D. Cowan, *Phys. Lett. A* **63**, 295 (1977).
32. M. B. Chowdhuri, S. Morita, M. Goto, H. Nishimura, K. Nagai, and S. Fujioka, *Plasma Fusion Res.* **2**, S1060 (2007).
33. R. Radtke, C. Biedermann, J. L. Schwob, P. Mandelbaum, and R. Doron, *Phys. Rev. A* **64**, 012720 (2001).